JOURNAL OF MATERIALS SCIENCE 28 (1993) 529–537

Comparison of shear-yielding modes in polycarbonate and a thermoplastic polyurethane

C. KAU*, A. TSE, A. HILTNER‡, E. BAER
Department of Macromolecular Science, and Center for Applied Polymer Research, Case Western Reserve University, Cleveland, OH 44106, USA

A thermoplastic polyurethane (PU) introduced by The Dow Chemical Company under the tradename Isoplast® possesses certain engineering properties that resemble those of polycarbonate (PC), including optical clarity, a glass transition of 140 °C, and comparable modulus and ductility. In this study, the shear-yielding behaviour at a circular hole was compared. Strain birefringence was used to analyse deformation in the linear elastic region. At higher stresses, optical microscope techniques were used to characterize the flow lines through the thickness of the plastically deformed region. Differences in shear-yielding behaviour were attributed to differences in the true stress–true strain relationship of the two materials. The true stress–true strain curve of PC exhibited a yield instability marked by a drop in the true stress. Shear yielding was described in terms of idealized elastic–plastic behaviour, and large-scale flow that accompanied yielding was responsible for the strong thickness dependence of shear yielding. The true stress–true strain curve of PU did not exhibit a true stress drop at the yield point. The primary features of shear yielding were consistent with elastic–plastic behaviour with work hardening; small local plastic strains resulted in more diffuse yielding that was not strongly dependent on thickness.

1. Introduction

Recently, a new family of injection-mouldable thermoplastic polyurethane materials has been introduced by The Dow Chemical Company under the tradename Isoplast® [1–3]. These MDI-based polymers are "live" in the sense that during normal processing they controllably depolymerize and repolymerize. Isoplast polyurethane (PU) possesses certain engineering properties that resemble those of polycarbonate (PC). It is optically clear with a glass transition temperature of about 140 °C, it is also ductile and deforms by shear yielding at ambient temperature with a yield strength that is about 15% higher than the yield strength of PC.

Although both PC and PU neck and cold-draw when extended in uniaxial tension, uniaxial tests can be seriously misleading in predicting notch sensitivity which involves failure at a crack tip where the stress state is triaxial. A more revealing comparison therefore requires a stress state where there is significant triaxiality. The sharp notch geometry is frequently used for observations in triaxial tension because the stress state approximates that at the tip of the propagating crack. On the other hand, the blunt notch is particularly attractive when the objective is to examine the deformation in a triaxial stress state while minimizing the tendency for crack growth. The importance of the plastic deformation zone that forms ahead of a stress concentrator such as a notch or hole has been recognized [4, 5]. When a notch results in large amounts of shear yielding, plasticity theory has proved useful for describing the instability. In particular, plasticity theory has provided a vehicle for understanding the relationship of the stress state, as determined by thickness, notch geometry, and applied load, to the shear-yielding mode.

The shear-yielding modes of notched polycarbonate sheet have been characterized under conditions that range from mostly plane strain to mostly plane stress [4]. Three shear-yielding modes are observed with increasing stress, namely core yielding, which is confined to the centre at the notch tip, the plane strain hinge shear mode, which is through thickness yielding on inclined planes above and below the notch, and finally the plane stress intersecting shear mode, where flow lines extend through the thickness at an angle to produce a necking effect. Like polycarbonate, PU is optically transparent, and methodology that relies on the optical microscope can be used to characterize the shear-yielding modes. In this study, the shear-yielding modes of PC and PU were compared, with particular attention to the effect of thickness on the plastic deformation zone that formed at a circular hole.

* *Present address*: Shell Development Company, Houston, TX 77251, USA
‡ Author to whom all correspondence should be addressed.

0022–2461

2. Materials and methods

2.1. Materials

A thermoplastic polyurethane (PU) with the tradename Isoplast® was supplied by The Dow Chemical Company in the form of ASTM D-638 Type I injection-moulded dumb-bell shaped tensile bars with thickness of 3.5 mm. Injection-moulded bars of Sinvet® 251 polycarbonate (PC) with the same geometry and 3.2 mm thick were supplied by Enichem Americas. When desired, thinner specimens were prepared by reducing the thickness with a milling machine. In some cases, a 1 mm radius circular hole was drilled in the centre of the 12.7 mm wide specimens.

The glass transition temperature was measured by differential scanning calorimetry. The Perkin–Elmer DSC7 instrument was used, the thermogram was recorded over the temperature range 30–300 °C with a heating rate of 20 °C min^{-1}.

2.2. Mechanical testing

Uniaxial tensile measurements were performed in an Instron machine; specimens were drawn to fracture at a strain rate of 5% min^{-1} at room temperature. An electronic strain gauge was attached to obtain accurate strain measurements for modulus determinations.

True stress–true strain curves of 3.5 mm thick PU and 3.2 mm thick PC were determined at room temperature by the grid method [6]. A grid pattern of about 3 × 3 lines mm^{-2} was vacuum-deposited on the gauge section of the specimens before deformation. The specimens were loaded at a crosshead speed of 5% min^{-1} to 15 mm displacement which was in the cold-draw region for both materials. The crosshead motion was stopped and photographs were taken of the width and the thickness along the gauge length. The true stress, σ_t and true strain, ε_t were calculated as

$$\sigma_t = \sigma_e w_0 t_0/(wt) \quad (1)$$

$$\varepsilon_t = (l - l_0)/l_0 \quad (2)$$

where the engineering stress, σ_e, was calculated as σ_e = force/(initial cross-sectional area), and w_0 and l_0 are the local grid width and length, respectively, before deformation, w and l are the local grid width and length after deformation, and t_0 and t are the thickness before and after deformation, respectively. The true stress–true strain curve before necking was obtained from the engineering stress–strain curve.

Specimens with a 1 mm radius circular hole were drawn in the Instron with a crosshead speed of 0.1 mm min^{-1} at room temperature. The region of the hole was photographed during deformation with the travelling optical microscope. In some cases, the specimen was loaded to the desired position on the stress–displacement curve, carefully unloaded and trimmed with a band saw. The specimen was then sectioned through the thickness with an Isomat cutting machine and the section viewed in the thickness direction in an Olympus model BH-2 optical microscope in the transmission mode under crossed polarizers.

2.3. Photoelastic effect

Specimens about 0.5 mm thick with a circular centre hole were photographed during deformation with the specimen located between the analyser and polarizer of the travelling optical microscope. Cyclic loading was performed with progressive increases in the displacement, a crosshead speed of 0.1 mm min^{-1} was used, and the photoelastic colour fringe patterns were photographed during loading and unloading.

3. Results and discussion

3.1. Mechanical properties

The PU was a clear, tough thermoplastic with a glass transition temperature of 140 °C, similar to that of polycarbonate. The mechanical properties were also similar to those of PC. The engineering stress–strain curves of the two polymers are compared in Fig. 1. Both exhibited a yield maximum that was accompanied by formation of a neck, followed by cold-drawing. The modulus of PU was about 10% lower than that of PC (Table 1), but the yield stress was significantly higher. As a result, necking occurred at a higher strain in PU than in PC. For example, when PU had just passed the upper yield point at an engineering strain of 13%, PC had already necked and was in the cold-draw region. In both materials, the neck propagated in a stable manner until fracture occurred, the maximum draw ratio of the necked material was the same, 1.8, in both cases.

Photographs of the propagating neck profile, Fig. 2, showed that narrowing of the gauge section occurred much more gradually in PU than in PC. The maximum in the engineering stress–strain curve that accompanied formation of the neck was correspondingly

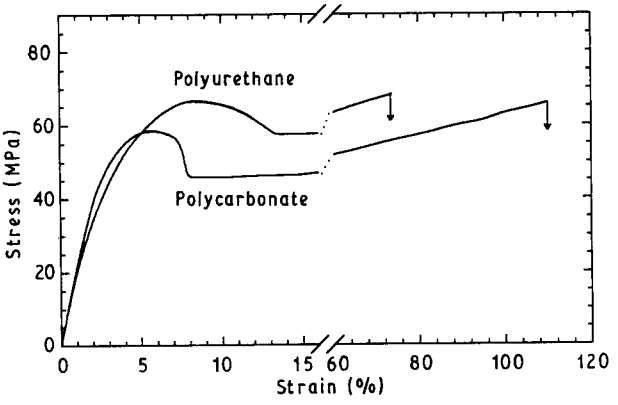

Figure 1 Engineering stress–strain curves of polycarbonate and polyurethane.

TABLE I Tensile properties of polycarbonate and Isoplast polyurethane

Property	Polycarbonate	Isoplast®
E (GPa)	2.3	2.1
σ_{yield} (MPa)	58.6 ± 0.6	69.2 ± 4.0
ε_{yield} (%)	6.8 ± 0.2	9.0 ± 0.5
$\Delta\sigma_{yield}$ (MPa)	12.7 ± 0.6	9.2 ± 0.2
$-(d\sigma/d\varepsilon)_{max}$ (MPa)	1630 ± 400	596 ± 94
$\sigma_{fracture}$ (MPa)	61.0 ± 8.0	65.8 ± 0.3
$\varepsilon_{fracture}$ (%)	106 ± 30	64 ± 10

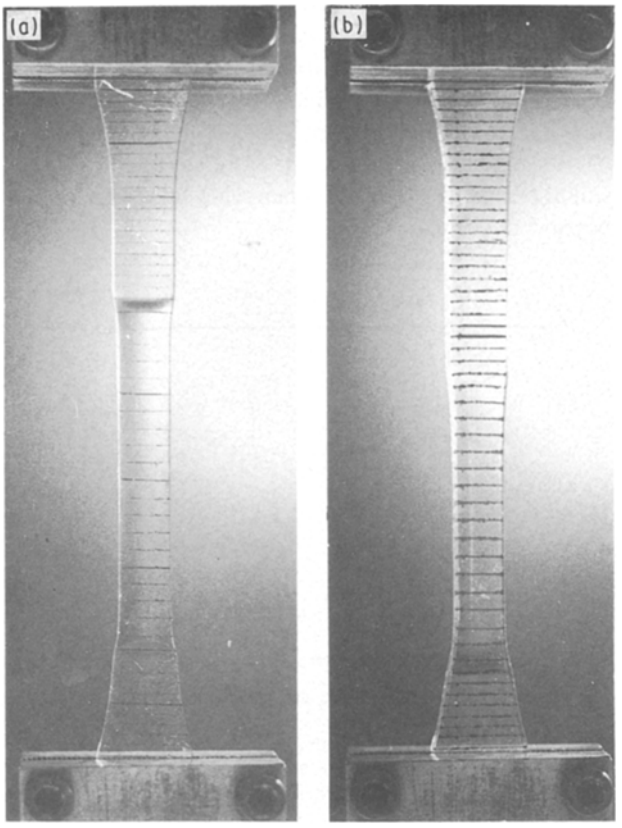

Figure 2 Photographs of the gauge section of tensile specimens that have necked and been partially drawn. (a) Polycarbonate, and (b) polyurethane.

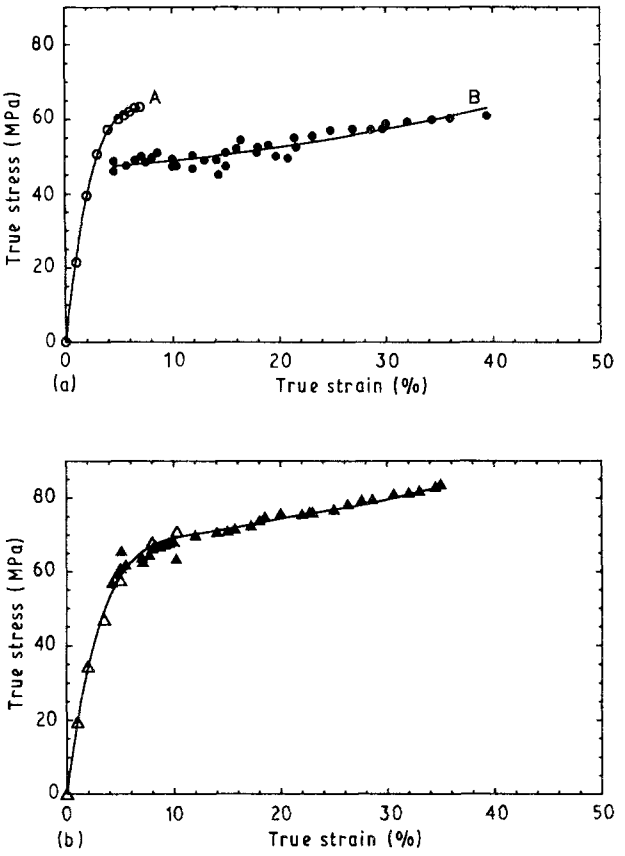

Figure 3 True stress–strain curves of (a) polycarbonate and (b) polyurethane.

much broader in PU. Two parameters have been used to describe the yield instability in the engineering stress–strain curve of polymers [7–10]. The index of cold-drawing, $\Delta\sigma_{yield}$, is defined as the difference between the yield stress, σ_y, and the cold-drawing plateau stress; the higher the value, the more easily the material draws. Secondly, the extent of tensile instability is given as the maximum negative slope of the stress–strain curve after the yield point, $-(d\sigma/d\varepsilon)_{max}$. These parameters were calculated from the engineering stress–strain curves of PU and PC and are included in Table 1. Smaller values of both parameters for PU reflected the more diffuse necking of this polymer.

The true stress–true strain curves of PU and PC are compared in Fig. 3. Two curves are plotted for each material: the true stress–true strain curve before necking obtained from the load–elongation curve, and the true stress–true strain curve of the steady-state propagating neck obtained by the grid method. Polycarbonate showed a yield instability, as has been reported by other investigators [6, 11, 12]. This behaviour is also exhibited by poly(ethylene terephthalate) [13], poly(vinyl chloride) [14, 15], and Nylon 6 and Nylon 66 [15]. When point A was reached at some location on the specimen, shear bands formed. Locally, material in the shear bands underwent a large extension from point A to point B. The material undergoing yielding can be described as elastic–plastic in that it is characterized by a true yield point at which flow ensues. In an unnotched tensile bar, yielding occurs at a defect; however, the location of yielding can be controlled by deliberately introducing an appropriate stress riser such as a notch. The true stress–true strain curve of PU did not have a noticeable drop in true stress at the yield. In this regard PU resembled the semicrystalline polymers, polyethylene and polypropylene [15, 16]. This behaviour is similar to the idealized stress–strain curve of an elastic–plastic material with work-hardening where the linear post-yield region has a positive slope.

3.2. Elastic shear strain in a thin sheet

It is often useful when comparing the mechanical behaviour of materials to localize deformation at a stress riser. The initial portions of the stress–displacement curves of PU and PC with a 1 mm radius centre hole are compared in Fig. 4; the curve did not depend on thickness in the range examined, about 0.5–3.5 mm. The initial slope was slightly higher for PC although a higher stress was attained in PU, features that were consistent with the un-notched stress–strain behaviour.

Small strains at a circular hole are conveniently measured in transparent materials by the photoelastic technique. The isochromatic fringe patterns were recorded as 0.52 mm thick PU and 0.62 mm thick PC were cyclically loaded to gradually increasing stresses indicated by positions 1–6 and 1′–8′ on the stress–displacement curves in Fig. 4. The isochromatic fringe patterns for PU and PC at positions 2 and 2′, respectively, on the stress–displacement curves are shown in Fig. 5. Because the two positions have

approximately the same displacement, the isochromatic fringe order is the same. The shapes of the two-dimensional fringe contours conformed with the elastic birefringence pattern for the circular hole geometry published in the literature [17].

The maximum shear strain, ε_{xy}, along the x-axis was calculated from the strain-optic equation

$$\begin{aligned} \varepsilon_{xy} &= \varepsilon_x - \varepsilon_y \\ &= \delta/(Kt) \end{aligned} \tag{3}$$

where δ is the relative retardation, K the strain-optical coefficient and t the specimen thickness. The strain-optical coefficient of PC was taken to be 0.125 [19] and, as a first approximation, the same value was used for PU. For comparison, the elastic shear stress was also calculated from the infinite plate solution for the circular hole [20]. Edge effects are reported to be negligible if the ratio of the width to hole radius is greater than 10:1 [20]. In this case, the ratio was 12.7:1.

The maximum shear strain ε_{xy} along the x-axis obtained from the fringe patterns at positions 1, 2 and 3 on the stress–displacement curve of PC and 1′, 2′ and 3′ for PU is plotted in Fig. 6. The correlation with the calculated elastic shear strain was excellent at positions 1, 1′, 2 and 2′. Some deviation was apparent at positions 3 and 3′; here the data points obtained from the fringe patterns lay slightly above the calculated elastic curve which would indicate some amount of non-linear behaviour. The deviation from the elastic solution only slightly preceeded the first detection of non-recoverable strain, the latter appearing as residual birefringence in specimens that had been loaded beyond position 3.

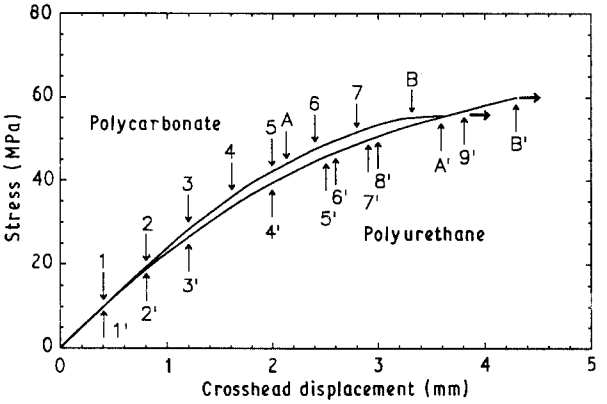

Figure 4 Stress–displacement curves of polycarbonate and polyurethane with a circular centre hole. The numbers refer to the positions at which the thin specimens were photographed, and the capital letters to positions at which the thick specimens were photographed.

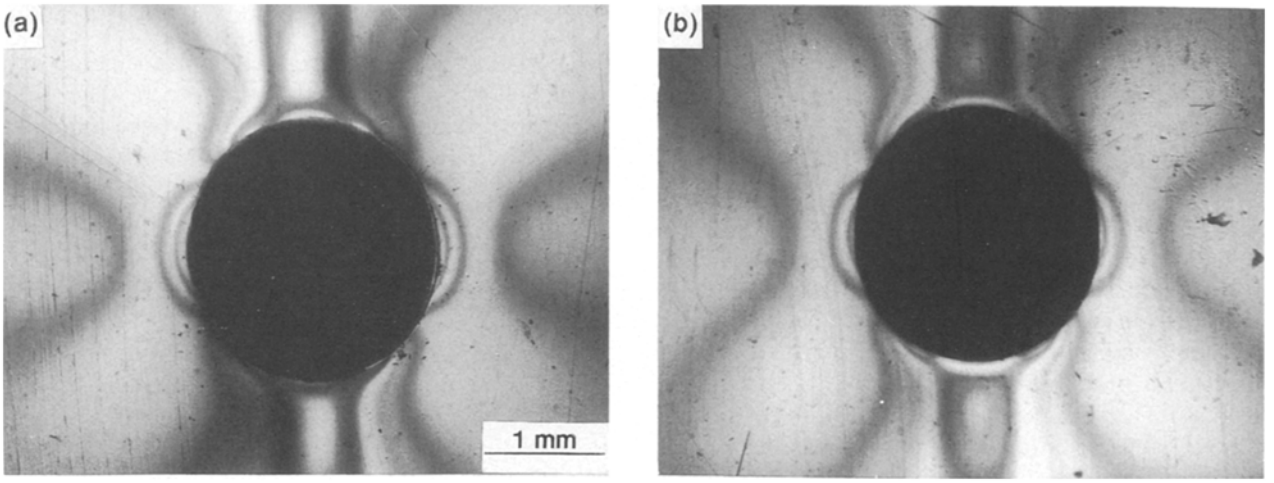

Figure 5 Isochromatic fringe patterns. (a) Polycarbonate loaded to position 2 on the stress–displacement curve, and (b) polyurethane loaded to position 2′ on the stress–displacement curve.

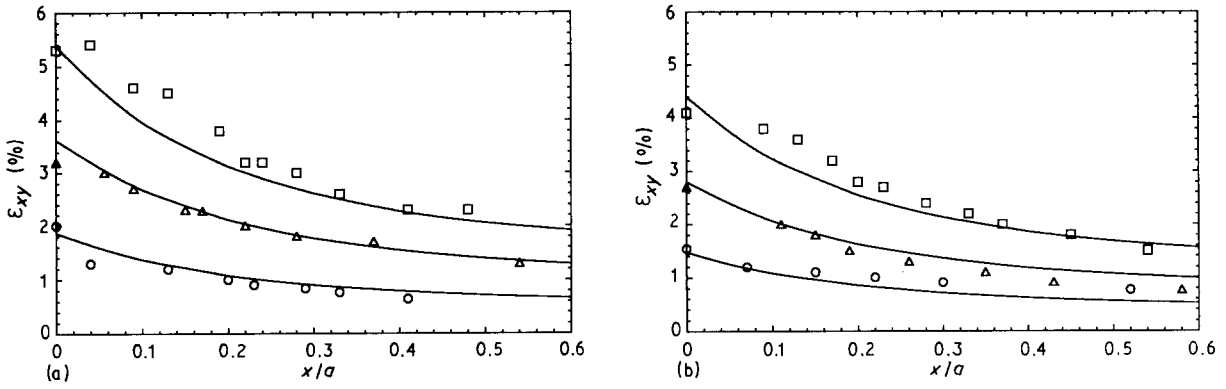

Figure 6 Maximum shear strain along the x-axis determined from isochromatic fringe patterns compared with calculated elastic shear strain. (a) Polycarbonate, and (b) polyurethane. σ_0: (a) (o) 10 MPa, (△) 20 MPa, (□) 30 MPa; (b) (o) 8 MPa, (△) 16 MPa, (□) 24 MPa.

3.3. Non-linearity

When specimens were loaded further past position 3 into the non-linear region of the stress–displacement curve, the isochromatic fringes became too numerous and indistinct to analyse; however, the residual birefringence when the specimens were unloaded was used to determine the extent of plastic yielding. To describe the behaviour when the elastic limit was exceeded, it was useful to estimate the remote loading conditions required for yielding at the hole root. Using the tensile yield stress from Table I and the von Mises yield criterion with the octahedral shear stress concentration factor at a circular hole of 1.26 in plane strain, the remote stress required for shear yielding of PC was calculated to be 22.6 MPa, compared to 26.0 MPa for PU.

From this calculation, the yield condition was achieved at the hole root in PC between positions 2 and 3 on the stress–displacement curve in Fig. 4. This was borne out experimentally when deviation of the measured shear strain from the elastic solution was first observed at position 3. When specimens were taken to still higher loads, the size and shape of the region that experienced plastic deformation were taken from the residual birefringence that remained after unloading. Residual birefringence in PC was concentrated in a small area at the root of the hole. The small area of residual birefringence visible at position 4 ($\sigma_0 = 0.64\sigma_y$), Fig. 7a, was somewhat larger at position 5 ($\sigma_0 = 0.76\sigma_y$), and at position 6 ($\sigma_0 = 0.84\sigma_y$) dark bands remained where macroscopic flow caused thinning at the hole root.

The yield condition was achieved in PU between positions 3′ and 4′, with a small area of residual birefringence observed at position 4′ ($\sigma_0 = 0.57\sigma_y$). The area of residual strain increased rapidly from positions 4′ to 8′ and changed from a circular shape to fan-shaped as PU was taken to higher stresses, Fig. 7b. At position 8′ ($\sigma_0 = 0.76\sigma_y$) the region of plastic strain extended well beyond the hole.

The contrast in plastic deformation of PC and PU that was evident soon after the yield stress was achieved at the hole root was attributed to the different true stress–true strain behaviour of the two materials. Comparing the residual birefringence patterns in Fig. 7, plastic deformation of PC was conspicuously concentrated in the region of the hole. Consistent with plasticity concepts, once the yield stress of the elastic–plastic material was achieved through the thickness, the strain at the hole was accommodated by necking with macroscopic flow [4]. The strain was much more broadly distributed in PU because work hardening prevented flow of PU and required local plastic strains to be small. With the plastic zone behaving as a region of gradually increasing modulus, strain at the hole was accommodated in the elastic region surrounding the plastic zone causing the plastic zone to gradually expand away from the hole.

3.4. Shear-yielding modes

3.4.1. Shear yielding in a thin sheet

When the shear yielding modes of PC and PU were compared at higher stresses it was again convenient to use a stress riser to localize deformation and also to control the degree of triaxiality. Without crossed polars, no deformation was visible in the optical microscope at the lower stresses where the strain birefringence measurements were made. At higher stresses, macroscopic shear yielding could be detected when the accompanying thinning of the specimen created regions of surface curvature which scattered light and appeared dark in the optical micrographs. The plane stress intersecting shear mode appeared in 0.62 mm thick sheet of PC as a pair of dark bands that curved away from the hole parallel to each other and perpendicular to the stress direction. The micrograph taken at position 7 on the stress–displacement curve shows the bands after they had grown some distance away from the hole, Fig. 8a. When the specimen was sectioned through the thickness at the position of the arrows and viewed in the polarizing optical microscope, a pair of broad intersecting flow lines was

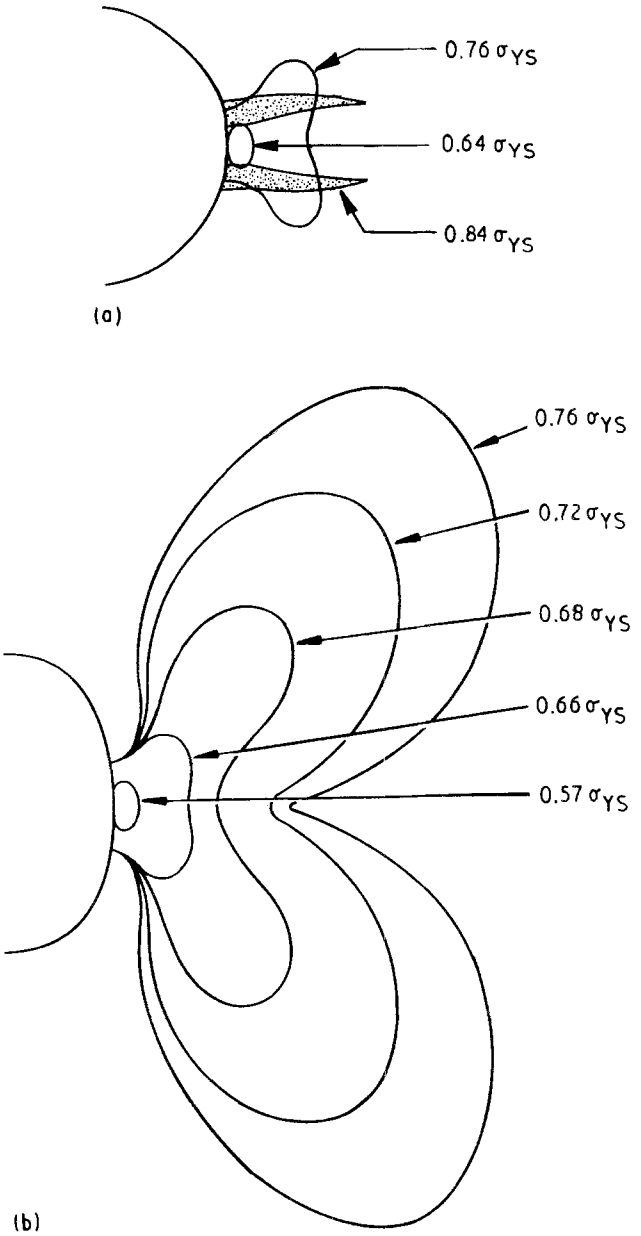

Figure 7 Residual strain birefringence patterns. (a) Polycarbonate after loading to positions 4–6 on the stress–displacement curve, and (b) polyurethane after loading to positions 4′–8′ on the stress–displacement curve.

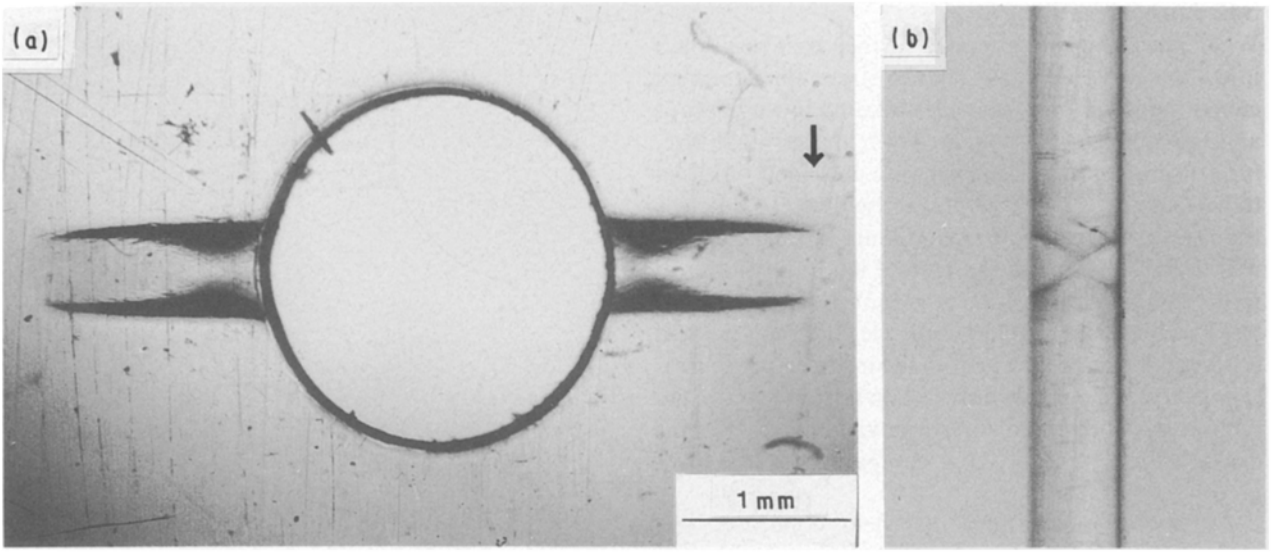

Figure 8 Polycarbonate 0.62 mm thick loaded to position 6 on the stress–displacement curve. (a) Front view, and (b) cross-section at the position of the arrows in (a).

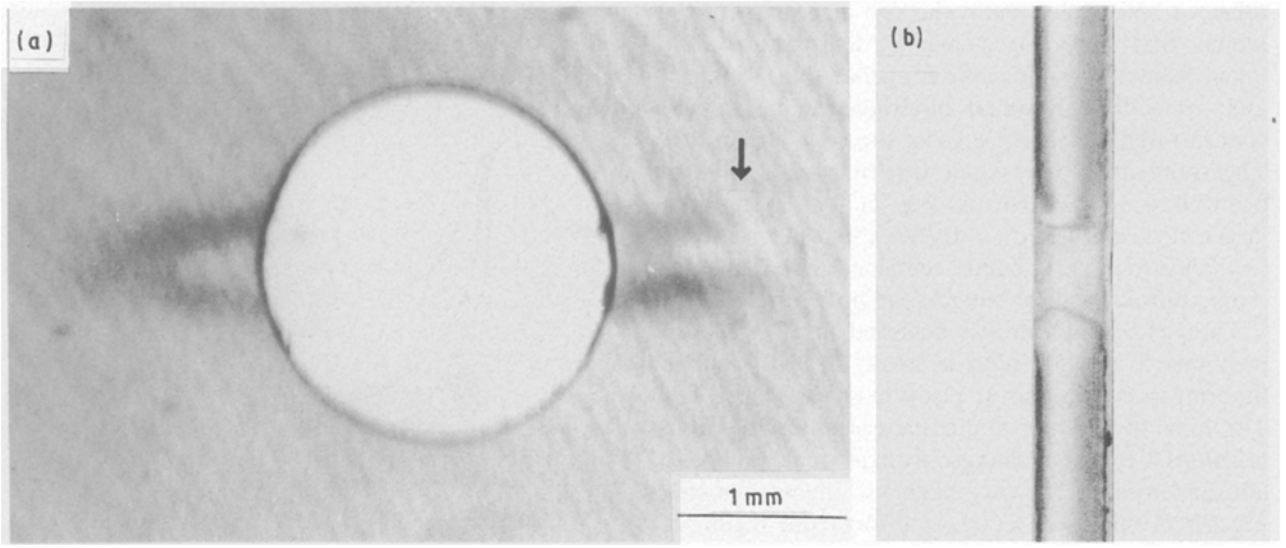

Figure 9 Polyurethane 0.52 mm thick loaded to position 9′ on the stress–displacement curve. (a) Front view, and (b) cross-section at the position of the arrow in (a).

visible; the flow lines extended through the thickness at an angle of about 53° to the loading direction, Fig. 8b. Surface curvature caused by the localized shear displacement and thinning of the specimen were visible; light scattering from the surface curvature where the flow lines intersected the surface produced the parallel dark bands in Fig. 8a.

The yielded zone of a PU specimen 0.52 mm thick that had been loaded to position 9′ on the stress–displacement curve in Fig. 4 was quite different in appearance from that of PC. The dark bands of the zone were more diffuse than in PC, Fig. 9a, and furthermore they extended only a short distance away from the hole. The dark bands did not grow in length as the stress increased, as had the intersecting shear bands in PC. Differences between the zones in thin sheet of PC and PU were also apparent when the zone of PU was viewed in cross-section, Fig. 9b. Instead of the flow lines of intersecting shear, the zone in PU appeared as parallel isostrain lines that extended through the thickness perpendicular to the loading direction.

3.4.2. Core yielding in a thick sheet

The stress–displacement curve of a thick sheet was the same as that of a thin sheet, but at higher stresses differences in the mode of shear yielding were apparent in the optical microscope. The first deformation that was visible in thick specimens of PC and PU was core yielding. This plane strain mode of shear yielding appeared in 3.5 and 3.2 mm thick specimens, respectively, as two families of intersecting α and β flow lines that grew out from the hole surface. The slip lines were most apparent when the focus was on the centre of the thickness at positions A and A′ on the stress–displacement curves in Fig. 4.

The distinct slip lines of core yielding in PC, Fig. 10a, clearly defined a plastic zone that conformed to the shape described by the Hill equation [20].

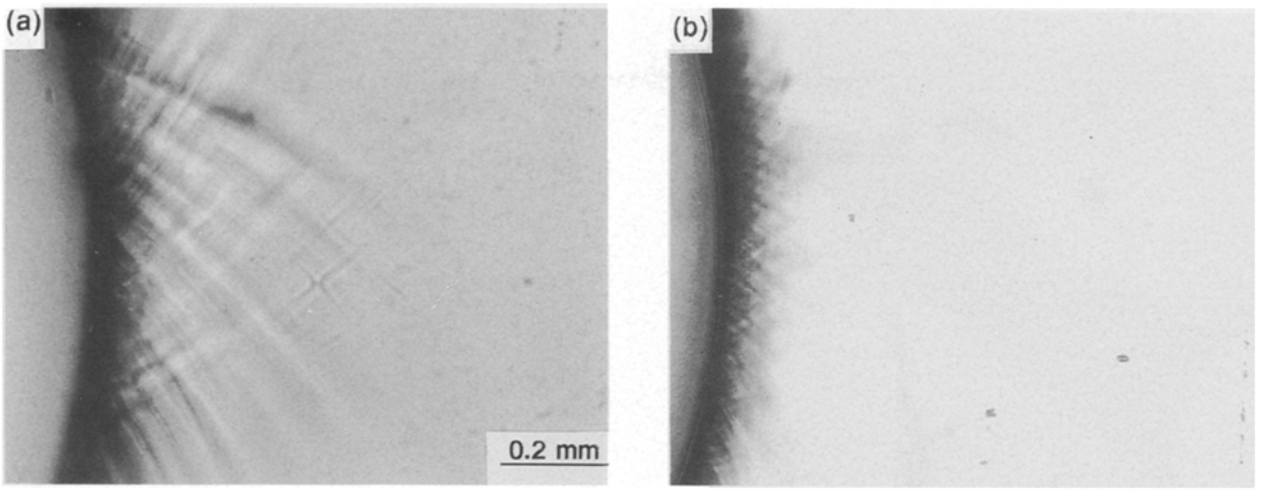

Figure 10 Core yielding. (a) 3.2 mm thick polycarbonate loaded to position A on the stress–displacement curve, and (b) 3.5 mm thick polyurethane loaded to position A′ on the stress–displacement curve.

Although the two families of curves appeared on first inspection to intersect at 90°, as predicted from a pressure-independent yield criterion, closer examination showed that the angle was about 85°. The angle between α and β slip lines, 2ψ, is related to the pressure-dependency through $\mu = \cos 2\psi$, where μ is the pressure coefficient in the modified von Mises yield equation [22, 23]. The value of $\mu = 0.076$ from the literature [24, 25] predicted that the two families of slip lines should intersect at an angle of 85.6°.

The slip lines of core yielding were less distinct in PU and could only be discerned in the optical microscope close to the notch surface, Fig. 10b. Growth of the slip lines out from the notch to form a clearly defined plastic zone with the characteristic Hill shape did not occur in this polymer. It was therefore difficult to determine whether the angle at which the slip lines intersected deviated significantly from 90°.

3.4.3. Shear yielding in a thick sheet

Plane strain core yielding cannot grow beyond a certain point being constrained by the surrounding elastic material, but the external surface provides a larger degree of freedom for extended yielding. The macroscopic shear yielding mode of PC is known to be strongly dependent on thickness [4]. When 3.2 mm thick PC was loaded to position B on the stress–displacement curve, core yielding was followed by the appearance of a pair of dark bands that grew out from the notch at an angle of 58° to the loading direction, Fig. 11a. The bands lengthened away from the hole as the stress increased. A cross-section at the position of the arrows in Fig. 11a showed parallel birefringent isostrain lines that extended through the thickness perpendicular to the loading direction when viewed in the polarizing optical microscope, Fig. 11b. The isostrain lines were concentrated at the positions, some distance above and below the notch, where the section cut through the dark bands. This mode of shear yielding was the through-thickness hinge shear mode described previously [4].

The hinge shear mode was not observed in thick sheet of PU. The small zone that formed in a 3.5 mm thick specimen loaded to position B′ on the stress–displacement curve appeared as diffuse dark bands in a small region directly in front of the hole, Fig. 12a. The dark bands did not grow in length away from the hole when the stress was increased, as had the hinge shear bands in PC. A cross-sectional view of the zone at the position of the arrows in Fig. 12a revealed parallel isostrain lines perpendicular to the loading direction, Fig. 12b; however, the fringes were concentrated in the region of the hole rather than some distance above and below the hole as in PC.

The yielded zone that formed in the 3.5 mm thick PU sheet was virtually indistinguishable in appearance from the zone in the thin sheet. Comparison of the cross-sectional views of thin and thick sheet in Figs 9b and 12b gave further confirmation that the form of the yielded zone in PU was essentially independent of thickness. In both cases, parallel isostrain lines extending through the thickness perpendicular to the loading direction were concentrated in a narrow region that measured about 0.5 mm, or about one-half the diameter of the centre hole.

3.4.4. Comparison of shear-yielding behaviour

Plasticity theory has been useful for describing the failure of certain ductile polymers such as PC [4] and PVC [26] that exhibit a yield instability with large plastic flow. The primary features of shear yielding including the effects of thickness can be described in terms of idealized elastic–plastic behaviour [4]. In the nearly plane strain condition, the dominating shear mode is hinge shear, which is through-thickness yielding on inclined planes above and below the hole. Intersecting shear dominates in the nearly plane stress condition; here yielding occurs through the entire thickness by slip along planes perpendicular to the principal stress that make an angle with the plane of the sheet. The transition from hinge shear to intersecting shear when the stress state is intermediate

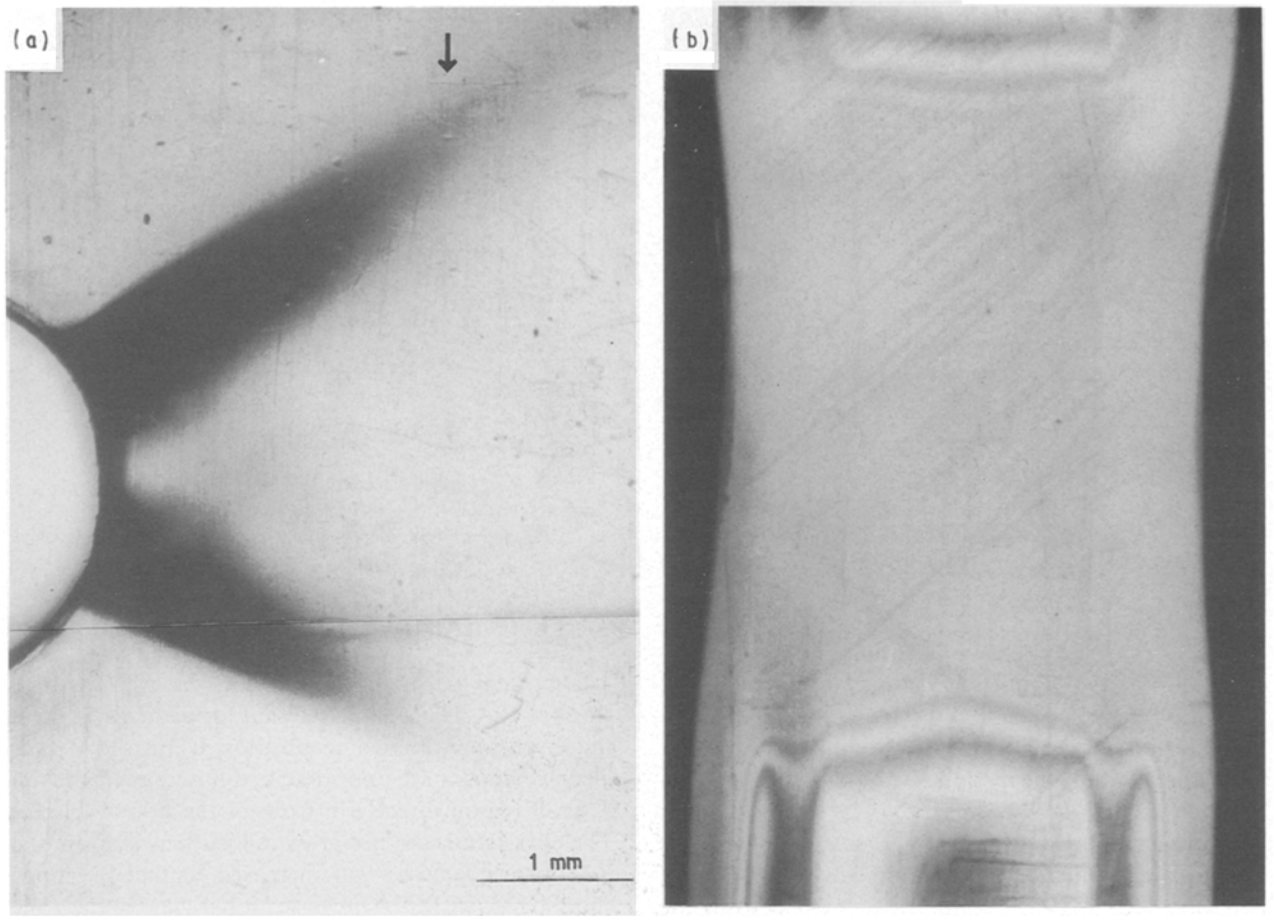

Figure 11 Polycarbonate 3.2 mm thick loaded to position B on the stress–displacement curve. (a) Front view, and (b) cross-section at the position of the arrow in (a).

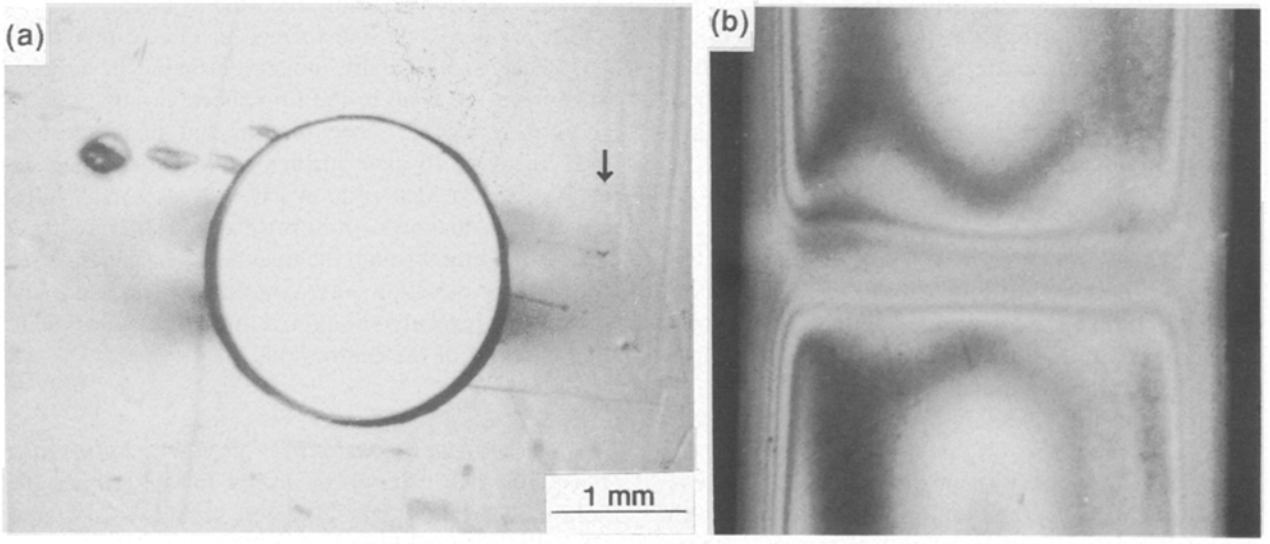

Figure 12 Polyurethane 3.5 mm thick loaded to position B′ on the stress–displacement curve. (a) Front view, and (b) cross-section at the positions of the arrow in (a).

between plane strain and plane stress has been described.

The true stress–true strain curve of PU did not exhibit a yield instability. Instead, the yield was characterized by a large change in modulus, behaviour that is more closely approximated as elastic–plastic with work-hardening. Plastic strains with work-hardening are locally small compared to plastic flow in the elastic–plastic material, and plastic deformation is consequently more diffuse. The diffuse yielding of PU was apparent in unnotched tensile tests, but the difference in the true stress–true strain behaviour was most evident when the yield condition was reached at a stress riser. When PC and PU specimens with a circular hole were loaded to comparable stress levels, for example to $\sigma_0 = 0.76\sigma_y$ (positions 5 and 8′ on the

stress–displacement curves), the residual birefringence extended over a much larger area around the hole in PU than in PC, well beyond the dark zone at the hole root (cf. Fig. 12a). The dark zone, which was produced by light scattering from surface curvature, revealed only the region where the strain was large enough to cause thinning of the specimen. The region of yielding with work hardening was actually much larger in PU and was probably more closely described by the residual birefringence than by the dark zone.

An important manifestation of the relatively small local plastic strains was the lessened dependency of yielding on the thickness with no major differences between yielding behaviour of thin and thick PU sheet. This suggested that a two-dimensional analysis would adequately describe yielding of both thin and thick PU sheet. A non-linear plane strain approach to large-scale yielding when the plastic zone is on the size scale of the stress riser, previously used to analyse the damage zone at a circular hole in rubber-modified polypropylene, was applicable [27]. The non-linear dependence of stress on strain was described by a gradually increasing numerical exponent, m, in the exponential relationship between stress and strain. The idealized stress–strain curve of an elastic–plastic material with work-hardening is a special case of non-linearity where an elastic region ($m = 1$) is followed by a plastic region characterized by a constant value of m. At a particular external load, the notched specimen has a specific stress distribution with the maximum stress at the root of the stress riser. Once the local stress at the root exceeds the elastic limit, plastic yielding with work-hardening occurs and a small plastic zone forms. Then every increment of external load causes expansion of the plastic, work-hardened zone that defines the elastic–plastic ($m = 1$) boundary. Assuming that the residual strain birefringence provided a qualitative image of the zone bounded by $m = 1$, the fan shape in Fig. 8b with dimensions on the size scale of the hole diameter was very similar in both size and shape to the zone described in the literature for the stress level $\sigma_0 = 0.76\sigma_y$ [27].

4. Conclusions

Shear yielding of a thermoplastic polyurethane (PU) at a circular hole during slow tensile loading has been compared with shear yielding of polycarbonate (PC). Although the PU closely resembles PC in certain of its engineering properties, differences in the true stress–true strain relationship result in significant differences in shear-yielding behaviour. The study leads to the following conclusions.

1. When strains are small, the shape of two-dimensional isochromatic fringe contours is satisfactorily described by a linear elastic analysis. Deviation from the elastic solution only slightly preceeds the first detection of non-recoverable strain when the yield condition is achieved at the root of the circular hole.

2. The true stress–true strain curve of PC exhibits a yield instability with a drop in the true stress. In comparison, the true stress–true strain curve of PU is characterized by a change in slope at the yield point but no drop in the true stress.

3. The primary features of shear yielding in PC can be described in terms of idealized elastic–plastic behaviour. Large-scale flow that accompanies yielding produces a strong thickness dependence characterized by the transition from the plane stress intersecting shear mode to the plane strain hinge shear mode.

4. The shear-yielding behaviour of PU shows features characteristic of an elastic–plastic material with work-hardening. Small local plastic strains result in more diffuse yielding that is not strongly dependent on thickness.

Acknowledgements

The authors thank Dr A. T. Chen, The Dow Chemical Company, Freeport, Texas, for providing the injection-moulded samples of Isoplast®. This work was generously supported by the National Science Foundation, grant no. DMR 91-00300.

References

1. P. J. MOSS, A. T. CHEN and B. S. EHRLICH, *SPE ANTEC* **35** (1989) 860.
2. R. J. PIERCE, *ibid.* **37** (1991) 2070.
3. B. S. EHRLICH, W. J. FARRISSEY, D. J. GOLDWASSER, R. W. OERTEL and K. ONDER, *J. Elast. Plast.* **16** (1984) 136.
4. M. MA, K. VIJAYAN, J. IM, A. HILTNER and E. BAER, *J. Mater. Sci.* **24** (1989) 2687.
5. A. TSE, E. SHIN, R. LAAKSO, A. HILTNER and E. BAER, *ibid.* **26** (1991) 2823.
6. G. BUISSON and D. RAVI-CHANDAR, *Polymer* **31** (1990) 2071.
7. P.B. BOWDEN and S. RAHA, *Phil. Mag.* **22** (1970) 455.
8. *Idem, ibid.* **22** (1970) 463.
9. A. SIEGMANN, L.K. ENGLISH, E. BAER and A. HILTNER, *Polym. Engng Sci.* **24** (1984) 877.
10. P. I. VINCENT, *Polymer* **1** (1970) 7.
11. W. A. SPITZIG and O. RICHMOND, *Polym. Engng Sci.* **19** (1979) 1129.
12. M. C. BOYCE and E.M. ARRUDA, *ibid.* **30** (1990) 1288.
13. N. BROWN and I.M. WARD, *J. Polym. Sci. A2* **6** (1968) 607.
14. P.J. FENELON, *Polym. Engng Sci.* **15** (1975) 538.
15. C. G'SELL and J.J. JONAS, *J. Mater. Sci.* **16** (1981) 1956.
16. G. MEINEL and A. PETERLIN, *J. Polym. Sci. A2* **9** (1971) 67.
17. A. NADAI, "Theory of Flow and Fracture of Solids", Vol. 1 (McGraw-Hill, New York, 1950) pp.175-274.
18. G. S. HOUSTER, "Experimental Stress Analysis" (Cambridge University Press, 1967) p.170.
19. N. J. MILLS, *J. Mater. Sci.* **17** (1982) 558.
20. S. TIMOSHENKO and J. N. GOODIER, "Theory of Elasticity", 3rd Edn. (McGraw-Hill, New York, 1968) p. 90, 92.
21. R. HILL, "The Mathematical Theory of Plasticity" (Clarendon, Oxford, 1950).
22. M. KITAGAWA, *J. Mater. Sci.* **17** (1982) 2514.
23. I. NARISAWA, M. ISHIKAWA and H. OGAWA, *ibid.* **15** (1980) 2059.
24. A. W. CHRISTIANSEN, E. BAER and V. RADCLIFFE, *Phil. Mag.* **24** (1971) 451.
25. P. B. BOWDEN and J. A. JUKES, *J. Mater. Sci.* **7** (1972) 52.
26. A. TSE, E. SHIN, A. HILTNER and E. BAER, *ibid.* **26** (1991) 5374.
27. C. J. CHOU, K. VIJAYAN, D. KIRBY, A. HILTNER and E. BAER, *ibid.* **23** (1988) 2533.

Received 3 March
and accepted 30 March 1992